FLUID & THERMAL ANALYSIS OF A MANIFOLD MICROCHANNEL HEAT SINK

Jarred Wilhite
NASA Glenn Research Center, Cleveland, OH 44135

Chirag Kharangate
Case Western Reserve University, Cleveland, OH 44104

ABSTRACT

A three-dimensional (3-D) numerical model has been developed to study the fluid flow and heat transfer through a manifold-microchannel (MMC) heat sink, a microfluidic cooling system designed as a heat dissipation solution for compact, high-powered electronic systems. An MMC consists of a 3-D manifold structure that distributes working fluid through alternating inlet and outlet manifold channels that guide the fluid to and from the microchannels, shortening the flow length and thereby, reducing the pressure drop across the system.

Wide bandgap semiconductors such as silicon carbide (SiC) are increasingly utilized due to their ability to enable smaller electronic devices and components to operate more efficiently at higher frequencies. These semiconductors can greatly benefit from the MMC, which can extract all the heat produced by compact, high-powered electronics, enabling them to achieve optimal performance. The MMC also utilizes an embedded cooling approach which allows for fabrication directly within SiC-based electronics, resulting in significant mass and weight savings and lower thermal resistance than conventional heat sink designs.

This paper outlines the methods used to conduct fluid and thermal analysis of different MMC configurations for flow parameters such as flow rate and inlet flow conditions. This study involves both steady state and transient thermal analysis as a gradually increasing heat flux is applied to the system over time, which is representative of the heat dissipation from the electronics over a given period. Results from the analysis show that the MMC is capable of effectively dissipating heat flux of ~100 W/cm^2 while maintaining considerably low pressure drop (< 1 kPa) and thermal resistance (< 1 K/W) for certain single-phase working fluids.

NOMENCLATURE, ACRONYMS, ABBREVIATIONS

f	friction factor
G	mass velocity [kg/m^2-s]
h_{ch}	microchannel height [μm]
h_{max}	maximum heat transfer coefficient [W/m^2-K]
L_{ch}	microchannel length [μm]
ΔP	pressure drop [kPa]
R_{th}	thermal resistance [K/W]
w_{ch}	microchannel width [μm]

INTRODUCTION

Advancements in technology continue to bring about designs for smaller, thinner, and lighter electronic devices and systems. As a result, the power density requirements for these electronics have increased significantly over the years to consistently meet consumer demands for power, speed, and performance. As these devices become smaller, more efficient thermal management methods must be implemented to maintain operating temperatures at acceptable levels and prevent premature failure due to overheating [1-2]. Thus, the objective of this project is to design and develop a manifold microchannel (MMC) heat sink as a compact, actively cooled heat dissipating solution to provide lightweight thermal management for advanced electronics with high power density requirements. With embedded cooling, the 3-D manifold structure and a finned microchannel array are both fabricated within SiC-based electronics which greatly reduces thermal resistance, size, and weight of the heat sink compared to traditional heat sink designs.

Figure 1(a) shows a schematic of the MMC heat sink which starts with fluid entering the manifold. The manifold is composed of multiple inlet-outlet pairs in which half of the manifold channels are inlets and the other half are outlets alternating along the length of the microchannels. The effective flow path is shortened as fluid flows from the manifold into the microchannels, resulting in a low pressure drop across the heat sink [2-3]. Also, the downward force of fluid flow into the microchannels interrupts the growth of thermal boundary layers, enabling greater net heat transfer coefficients with the developing region of flow [2]. Then, fluid flows through the outlet manifold channels, exiting the MMC. This overall process allows the MMC to achieve high heat transfer rates while maintaining low pressure drops across the heat sink, resulting in less pumping power needed than for a traditional microchannel heat sink [2-4].

Many numerical studies on the MMC have demonstrated its capability to significantly reduce the pressure drop compared to conventional heat sinks [5-7]. Recently, experimental studies have been done to validate the thermal-fluidic performance of the MMC, including Jung et al [4], who investigated an embedded silicon microcooler at various flow rates and conditions with water as the working fluid [3]. The current work utilizes additive manufacturing techniques and similar bonding strategy to construct a SiC-based MMC which will be discussed in the following section.

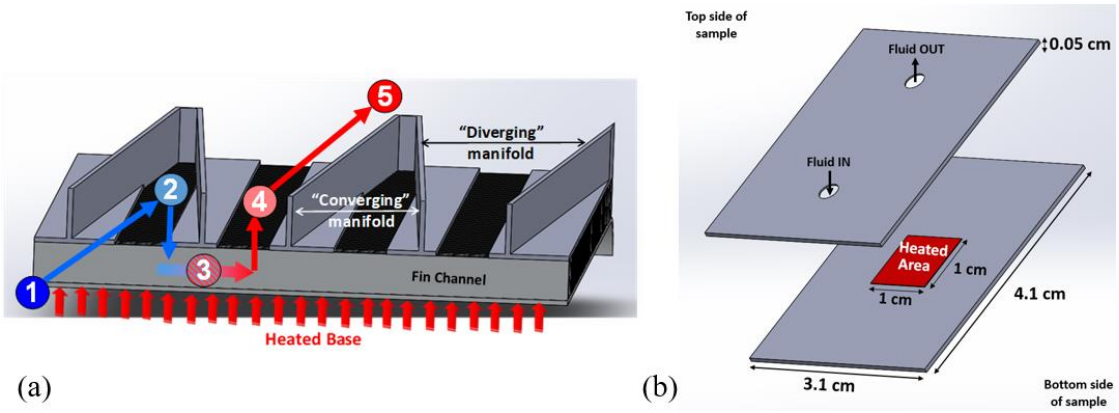

Figure 1. (a) MMC schematic showing the fluidic routing; (b) schematic of MMC sample.

PROJECT APPROACH

The MMC is fabricated within two SiC wafers, each 350-um thick as shown in Figure 1(b). The 3-D manifold and the fluid inlet and outlet ports are fabricated in the top wafer, while the microchannels are etched in the bottom wafer at a channel height of at least 100 μm. The wafers are then bonded together to form the final MMC sample, which will be integrated into a flow loop for testing. The MMC apparatus also includes a thin film heater to be deposited on the backside of the MMC to simulate heat dissipation from the electronics (~100 W/cm^2).

Microfabrication

Microfabrication for this project is being conducted in the Microsystems Fabrication Laboratory (MSL) at NASA's Glenn Research Center. The MSL contains an ISO 5 & 6 cleanroom facility with various types of machinery used to fabricate prototype SiC semiconductor integrated circuit electronics and sensors for use in harsh environments [8]. Various steps are taken to prepare the wafer surface for fabrication starting with bakeout to remove any external contaminants. A three-sample layout was drawn for each manifold and microchannel configuration as shown in Figure 2(a). Photomasks were created from these drawings which were then used to pattern each wafer. This included applying a thin, uniform photoresist coating on the wafer, using machines to conduct photolithography processes to transfer patterns from the photomask onto the wafer as shown in Figure 2(b). This process is followed by nickel electroplating in which the wafer is coated with a thin, 10-μm layer of nickel to protect the unetched surfaces of the wafer.

The wafers are fabricated using an Oxford Instruments Inductively Coupled Plasma (ICP) Reactive Ion Etcher (RIE) to conduct plasma etching of the wafer with high selectivity and excellent profile control for high etch uniformity [9]. Using a 50/50 mixture of SF_6/Argon, the ICP RIE produces uniform, high-density plasma etching to achieve high etch rates (~1 μm/min) due to the high ion density (≥ 10^{11}/cm^3) and high radical density while operating at low pressures (10-90 mTorr) [9-10]. Lower pressures facilitate the transport of etchants into and out of narrow trenches, providing smooth surfaces with no residue upon fabrication [10]. Fabrication is followed by dicing the wafers along the perforations to cut each sample from the wafer. The low-chemical vapor deposition chamber will be used to form a eutectic bond between the wafers.

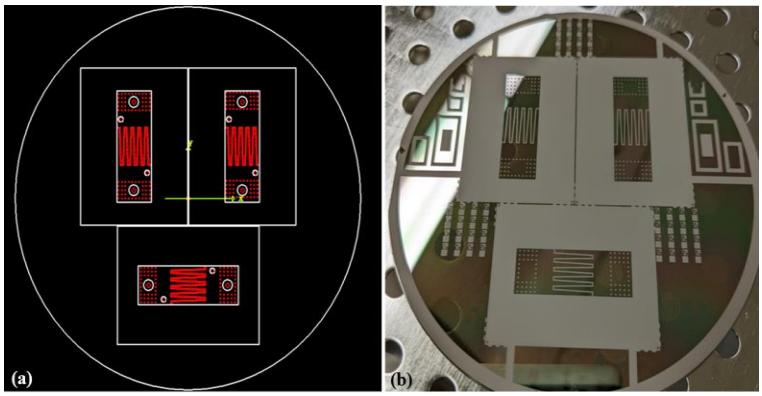

Figure 2. (a) Photomask drawing of manifold pattern; (b) Wafer patterned after photoresist application.

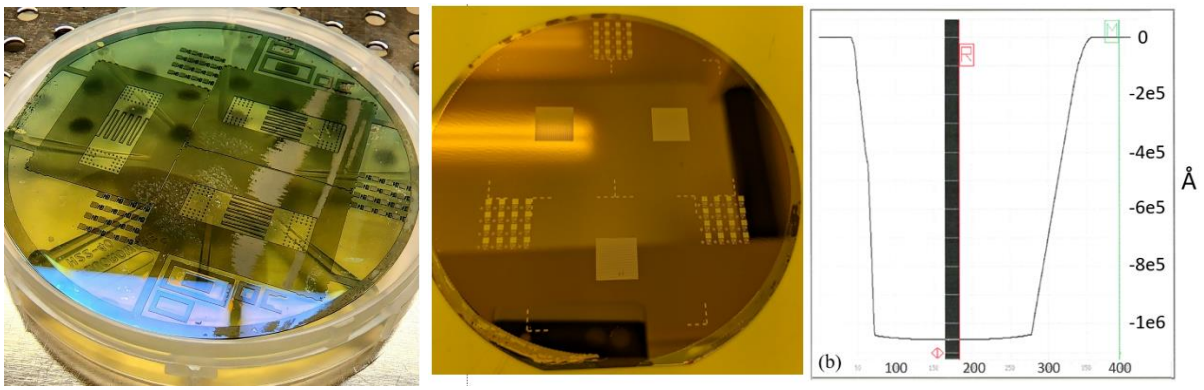

Figure 3. (a) Wafer with fabricated manifold pattern; (b) wafer with fabricated microchannels; (c) surface profilometer reading.

Figures 3(a) and 3(b) show the wafers with fabricated manifold and microchannel patterns, respectively. The surface profilometer reading is shown in Figure 3(c) which confirms that the microchannels on the wafer in Figure 3(b) are etched at a depth of 100 μm, or 10^6 Å. Moreover, the flatness in the profilometer curve indicates the smoothness of the fabricated surface which is a very desirable quality when etching.

Modeling

Reduced order modeling was done to predict the thermal performance of the MMC for various configurations. This modeling effort involved using equations of state, geometric parameters of the MMC, and flow parameters to model and simulate single-phase fluid flow through the device. Assuming ambient pressure at the inlet, the reduced order model utilizes the Reference Fluid Thermodynamic and Transport Properties (REFPROP) function to determine the corresponding inlet temperature for various working fluids of the MMC. These inlet conditions along with Prandtl number, Pr, and parameters such as hydraulic diameter D_h, microchannel length, L_{ch}, width, w_{ch}, and height, $h_{ch,}$ were used to calculate Nusselt number, Nu as follows [11]:

$$Nu = 0.1165\left(\frac{D_h}{L_{ch}}\right)^{0.81}\left(\frac{h_{ch}}{w_{ch}}\right)^{-0.79} Re^{0.62} Pr^{0.33} \quad (1)$$

Calculations for both Reynolds and Nusselt number ($Re \approx 1300$, $Nu \approx 6$) confirmed laminar flow through the MMC as intended for this project. Key parameters such as single-phase upstream pressure drop, $\Delta P_{sp,u}$ [10], thermal resistance, R_{th} and maximum heat transfer coefficient, h_{max} were calculated using the following relations:

$$\Delta P_{sp,u} = \frac{2fG^2 L_{ch}}{\rho D_h} \quad (2)$$

$$R_{th} = \frac{T_w - T_{in}}{q" L_{ch} w_{ch}} \quad (3)$$

$$h_{max} = \frac{Nu * k}{D_h} \quad (4)$$

where density, ρ and mass velocity, G are used to find $\Delta P_{sp,u}$ which is calculated by dividing the flow rate by h_{ch} and w_{ch}. Single-phase friction factor, f is another parameter used to calculate pressure drop and it is determined using an empirical formula that incorporates the aspect ratio of the microchannels [12]. The model determines pressure drop at different instances throughout the length of the microchannels using an equation very similar to Eq. (2). Thermal parameters that are used in these calculations include wall and inlet temperature, T_w and T_{in}, respectively, applied heat flux, q'', and thermal conductivity.

The reduced order analysis was further validated using a 3-D numerical model developed in Ansys Fluent which includes the full geometry of the MMC sample. Figure 4 shows the MMC geometry that was used for both the thermal and fluid models. The top face of the sample is hidden to show the test section area (highlighted in green) where fluid flows through the manifold and microchannels from the inlet to the outlet port. The Fluent model was used to determine the pressure drop across the heat sink while a thermal model of the MMC was created using Ansys Mechanical to conduct steady state and transient thermal analysis. Inlet conditions for these models include water entering the inlet at ambient pressure and inlet temperature of 25°C at 0.18 m/s. A heat flux of 100 W/cm^2 was applied on the heater surface on the backside of the sample, which is consistent with the reduced order model.

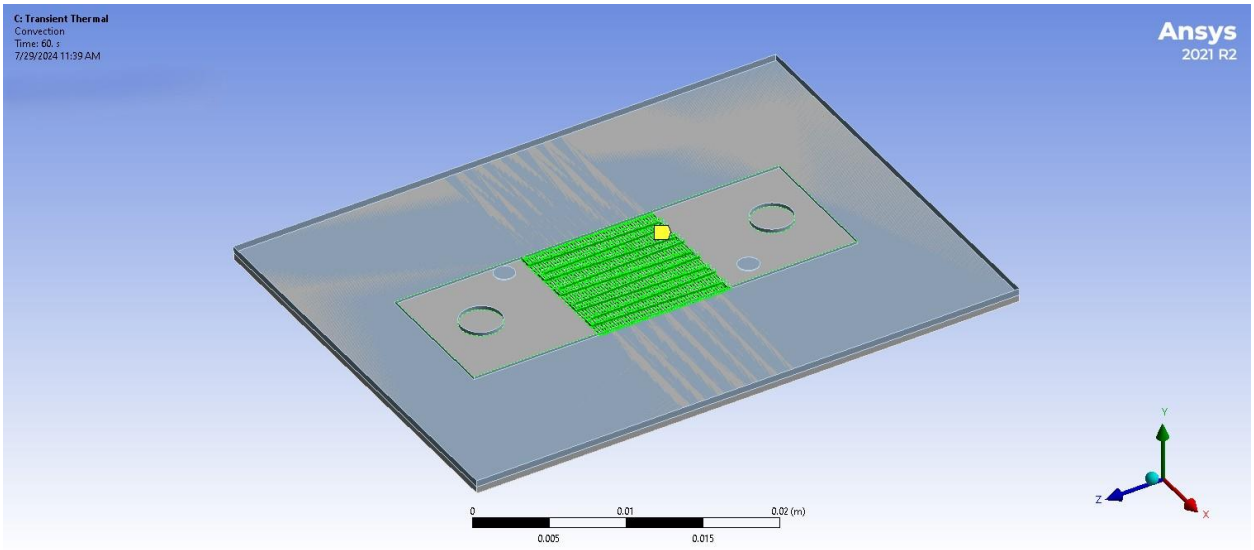

Figure 4. MMC geometry showing the test section area (green)

Results

The Fluent analysis involved distinguishing between fluid and solid domains. The test section area was established as the fluid domain, while the remaining faces of the sample and thin film heater were established as the solid domain. Using k-omega SST, the Fluent model was used to run a steady state simulation of the internal flow of water through the MMC. Considering the properties of water at ambient pressure, such as thermal conductivity, density, and specific heat, Fluent results in Figure 5 show a pressure drop of 0.143 kPa as the fluid flows from the inlet to the outlet.

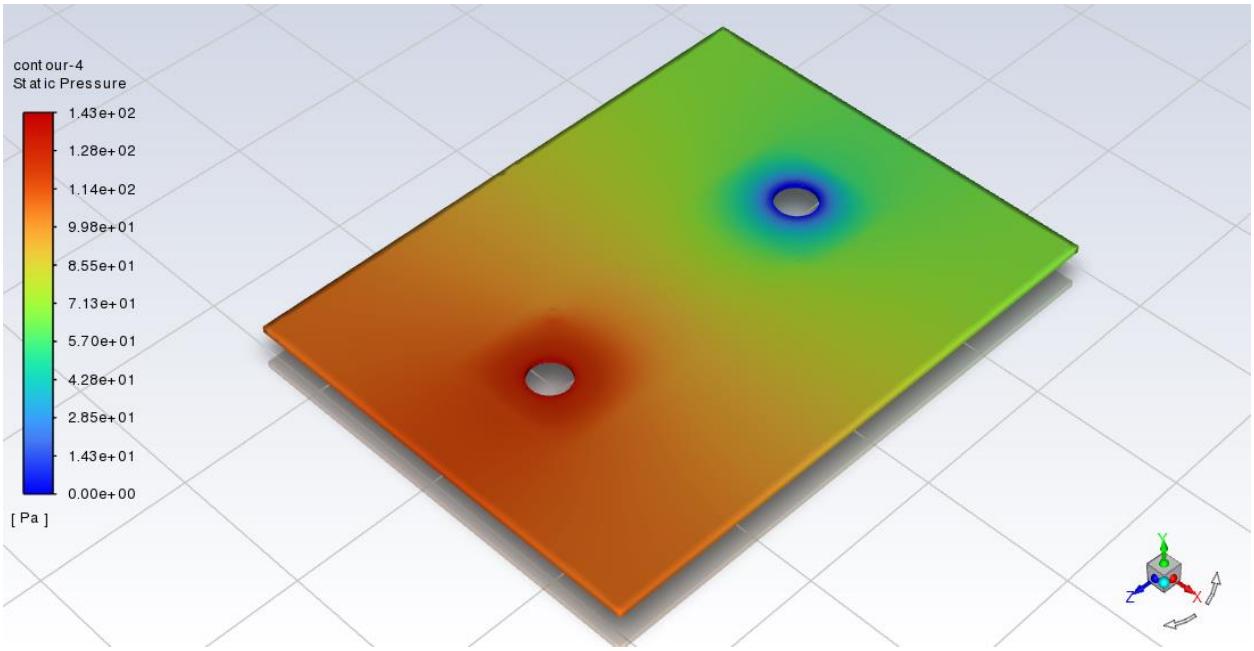

Figure 5. Fluent analysis plot showing the pressure drop across the MMC.

The post-processed plots from the steady state thermal analysis are shown in Figure 6, showing the temperature distribution along the top and bottom sides of the MMC sample. As fluid flows from the inlet at 25°C and is distributed throughout the MMC, it reaches temperatures of 65-70°C near the outlet. This rise in temperature is expected since the fluid absorbs heat while flowing through the heated microchannels. As the heater reaches a maximum temperature of 113.1°C, the surface temperature across the wafer increases, especially near the 1cm^2 heated surface area. Despite this, the water remains well below 100°C as it flows through the MMC, indicating that the MMC can effectively dissipate heat when utilizing single-phase water as the working fluid for the specified inlet conditions.

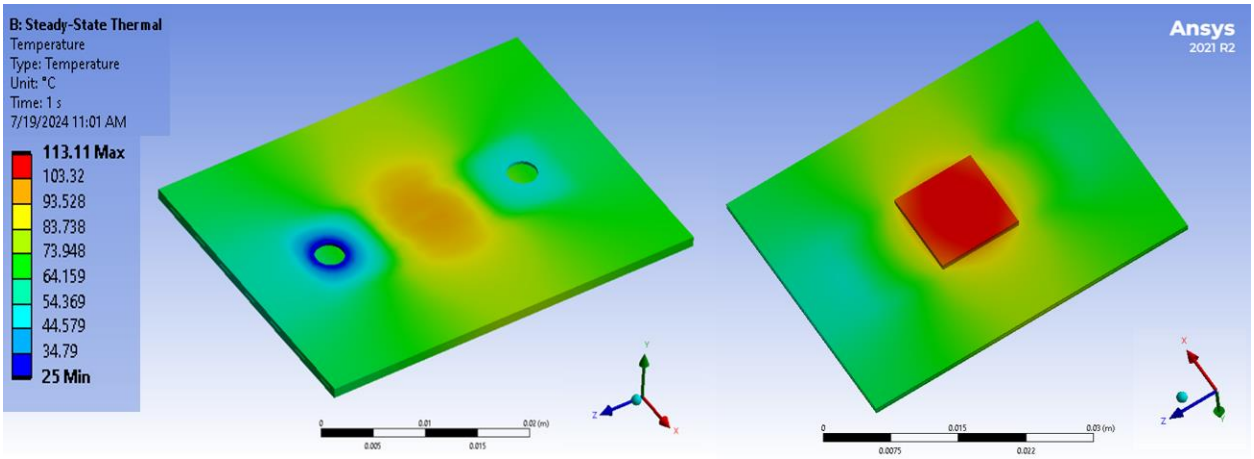

Figure 6. Steady state thermal analysis plot for the MMC; top side and bottom side views.

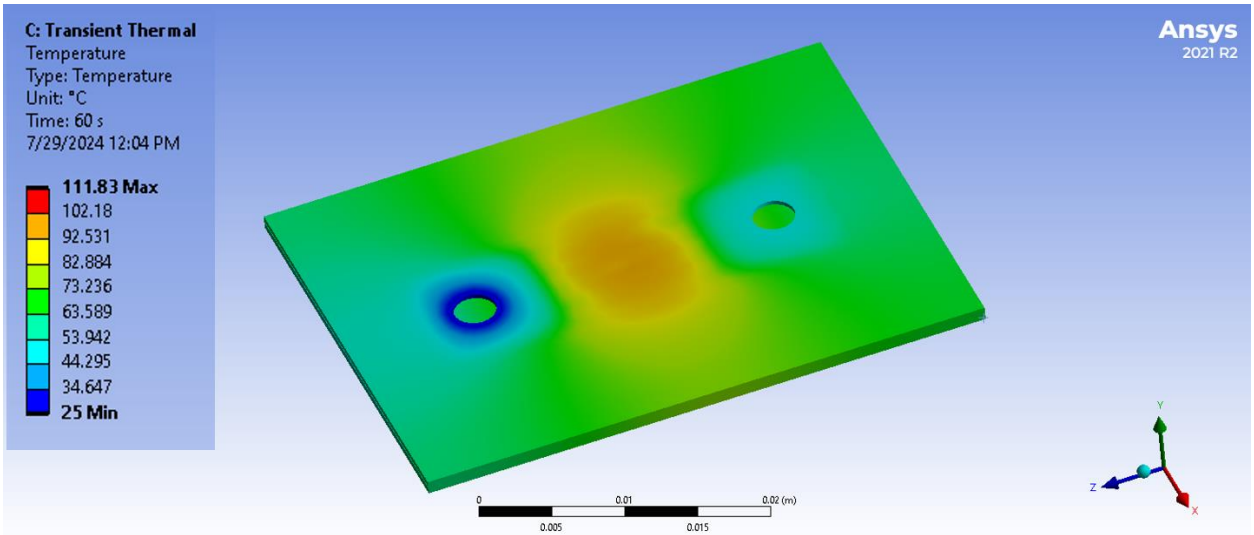

Figure 7. Transient thermal analysis plot for the MMC at t = 60 s (top side).

This is further confirmed by the transient thermal analysis, which uses the same inlet conditions as in the steady state case. Figure 7 shows the temperature distribution across the MMC assuming the heater reaches full power at a final time step of 60 seconds. The heater response can be as rapid or as gradual as desired based on the heater control that will be used in flow loop testing. As expected, the response is very similar to that shown in the steady state case in Figure 6, further validating that water remains single phase (~70°C) as it flows through the MMC.

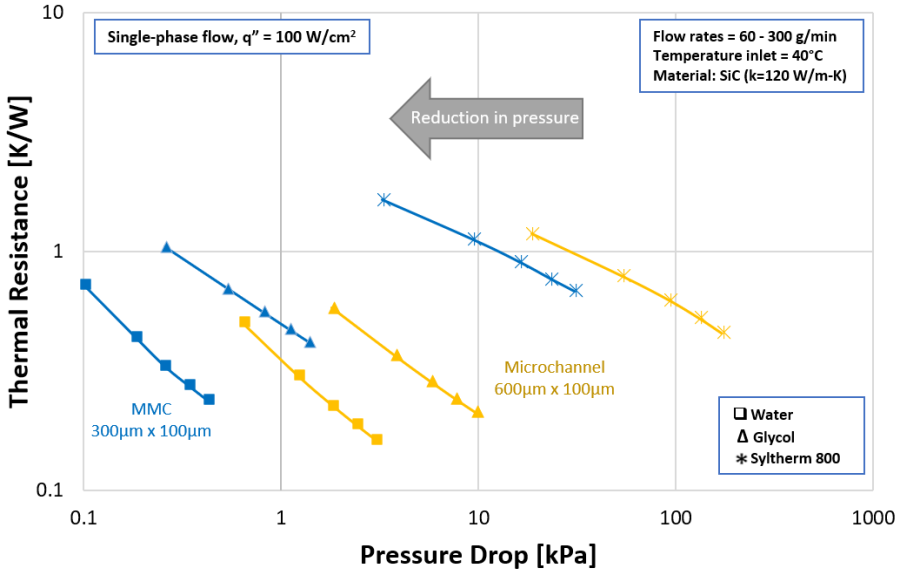

Figure 8. R_{th} vs. ΔP: MMC vs. microchannel heat sink for various working fluids.

The plots shown in Figures 8-11 are generated from the reduced-order analysis. Figure 8 shows that for various single-phase working fluids, the MMC provides a noticeable reduction in pressure

drop compared to the traditional microchannel heat sink, resulting in less pumping power requirements for the system. Despite the MMC being limited to a channel height of 300 μm compared to a 600 μm channel height for the traditional microchannels, the MMC is still capable of reaching lower thermal resistances as the flow rate is increased from 60 to 300 g/min.

Figure 9 shows the maximum heat transfer coefficients which are calculated using Eq. (4) and plotted over a range of flow rates from 100 to 400 g/min. The working fluids in this plot are water, R1233zd, and R1234yf. The latter two working fluids are refrigerants that are non-ozone depleting (ODP = 0) with an ultra-low global warming potential (GWP ≤ 1). These fluids belong to a new generation of low-pressure refrigerants that are meant to replace traditional HFC refrigerants like R134a and R245fa which have relatively higher GWPs of 1430 and 1020, respectively [12].

The calculations made to obtain plots for Figures 9-11 assume an exit temperature, T_{exit} of each working fluid at 1°C below their respective boiling points to determine the MMC performance in a conservative analysis. REFPROP was used to find the corresponding inlet conditions, P_{in} and T_{in} to obtain the desired T_{exit}. As expected, the maximum heat transfer coefficient, h_{max} for each fluid increases with flow rate. The plots show that despite different working fluids being used, the MMC consistently reaches higher h_{max} values, further demonstrating its benefits over the traditional microchannel heat sink.

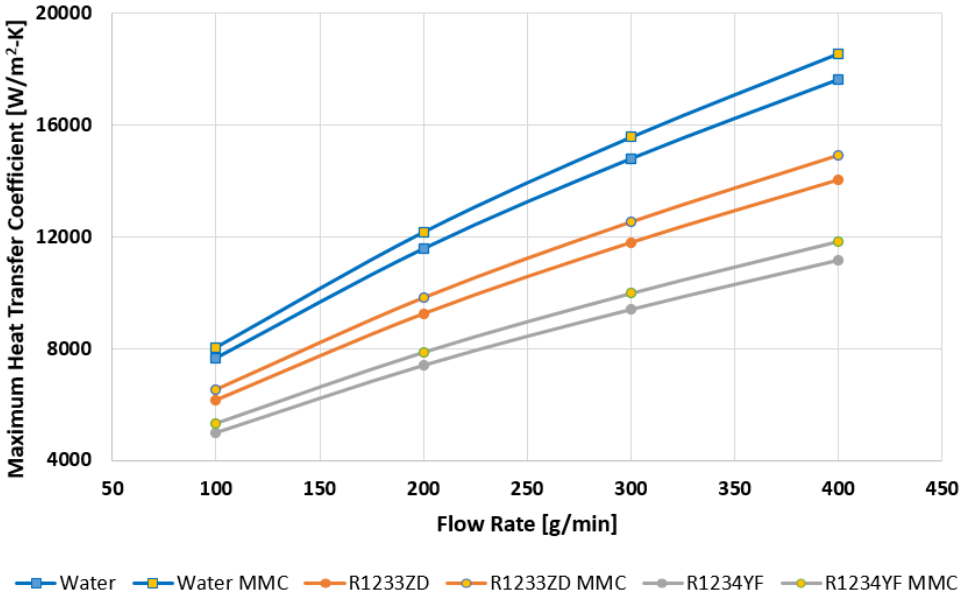

Figure 9. Maximum heat transfer coefficient: MMC vs. microchannel heat sink for various working fluids.

The reduced order analysis was also done to compare different MMC configurations as shown in Figures 10 & 11 for water and R1233zd, two working fluids that will be used during flow loop testing of the MMC. These configurations have varying channel height, h_{ch} of 100, 200, and 300 μm, with a constant channel width, w_{ch} of 100 μm. Figure 10 shows the pressure drop plotted over the flow rate range of 100-400 g/min. Each configuration shows the pressure drop to increase with flow rate, which is consistent with results obtained in previous MMC studies [1, 4]. There is a

noticeable decrease in pressure drop as the channel height is increased to the maximum h_{ch} of 300 µm, which illustrates the benefits that can be achieved with fabricating the microchannels of the MMC at a greater height. Figure 11 plots the thermal resistance over the same range of flow rates. While the thermal resistance is relatively low for each working fluid and each configuration, the MMC with h_{ch} of 300 µm shows slightly greater thermal resistance. The trends in Figures 10 & 11 show that a balance must be reached between each parameter to achieve optimal MMC performance.

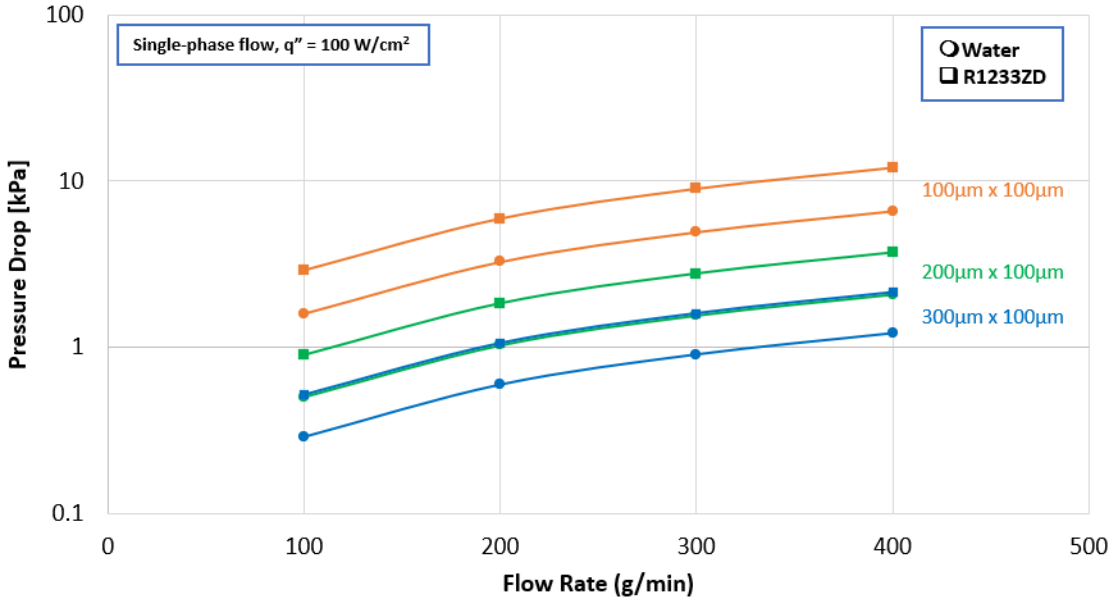

Figure 10. Pressure drops vs. flow rate for different MMC configurations.

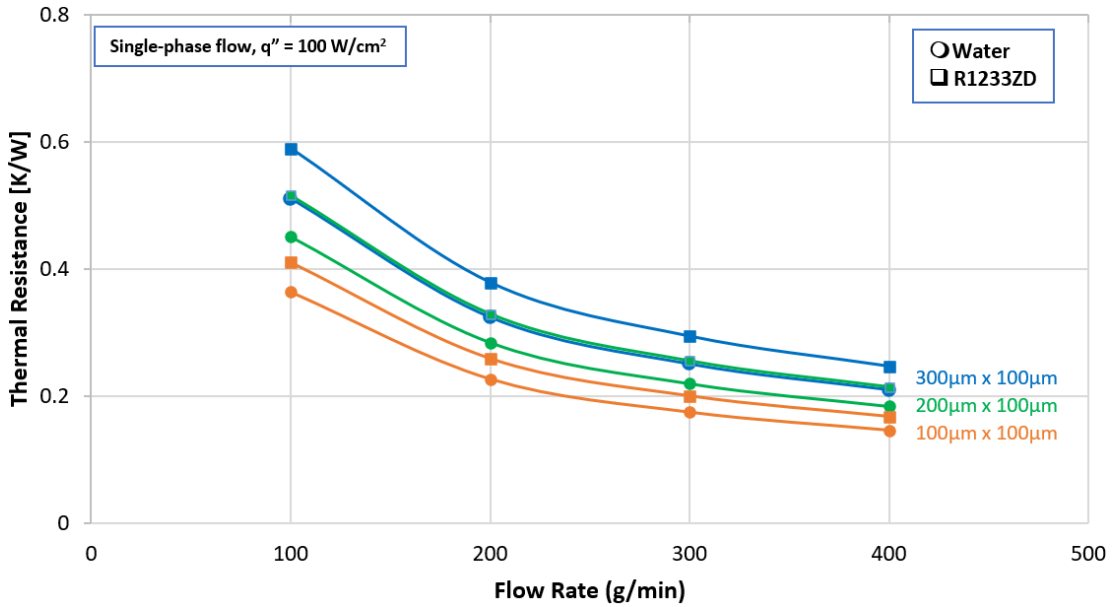

Figure 11. Thermal resistance vs. flow rate for different MMC configurations.

CONCLUSIONS

The MMC is a lightweight, actively cooled heat dissipation solution that can be used to benefit compact electronics with high power density requirements. Fluid and thermal analyses, as well as reduced order analysis were used to demonstrate the capabilities of a SiC-based MMC. Results from these analyses verify that the MMC can meet chip-level heat dissipation targets of 100 W/cm^2 while maintaining low thermal resistance (< 1 K/W) and very low pressure drops (< 1 kPa) for certain single-phase working fluids. Channel height is also a key factor in the MMC performance.

ACKNOWLEDGEMENTS

The authors would like to thank the NASA GRC Microsystems Fabrication Laboratory engineers and technicians who have supported MMC fabrication and manufacturing for this project.

REFERENCES

[1]Zhang, Z., Wang, X., Yan, Y., "A review of the state-of-the-art in electronic cooling", e-Prime – Advances in Electrical Engineering, Electronics, and Energy, 2021.

[2]Kong, D., Kim, Y., Kang, M., Song, E., Hong, Y., Kim, H. S., Rah, K. J., Choi, H. G., Agonafer, D., & Lee, H. "A holistic approach to thermal-hydraulic design of 3D manifold microchannel heat sinks for energy-efficient cooling." Case Studies in Thermal Engineering (28), 2021.

[3]Xie, X., Liu, Z., He, Y., Tao, W., "Numerical study of laminar heat transfer and pressure drop characteristics in a water-cooled minichannel heat sink", Applied Thermal Engineering (29), 2009.

[4]Jung, K.W., Kharangate, C.R., Lee, H., Palko, J., Zhou, F., Asheghi, M., Dede, E.M., Goodson, K.E. "Embedded cooling with 3D manifold for vehicle power electronics application: Single-phase thermal-fluid performance", Int. J. Heat Mass Transfer, 2019, 1108-1119.

[5]Harpole, G.M, Eninger, J.E., "Micro-channel heat exchanger optimization", 7th IEEE SEMI-THERM Symposium, 1991, 59–63.

[6]Boteler, L., Jankowski, N., McCluskey, P., Morgan, B., "Numerical investigation and sensitivity analysis of manifold microchannel coolers", Int. J. Heat Mass Transfer, Vol. 55, 2012, 7698-7708.

[7]Cetegen, E., "Force Fed Microchannel High Heat Flux Cooling Utilizing Microgrooved Surfaces", University of Maryland, College Park, 2010, Ph.D. Thesis.

[8]Neudeck, P. "Microsystems Fabrication Laboratory", NASA Glenn Research Center, 26 Sept. 2022. https://www1.grc.nasa.gov/facilities/microfab/

[9]"Reactive Ion Etching (RIE)", Oxford Instruments Plasma Technology. 2024. https://plasma.oxinst.com/technology/reactive-ion-etching

[10]Beheim, G., "Deep Reactive Ion Etching for Bulk Micromachining of SiC", CRC Press, 2002.

[11]Kim, S.-M., Mudawar, I. “Consolidated method to predicting pressure drop and heat transfer coefficient for both subcooled and saturated flow boiling in micro-channel heat sinks”, Int. J. Heat Mass Transfer, Vol. 55, 2012, 3720-3731.

[12]Longo, G., Mancin, S., Righetti, G., Zilio, C., “Boiling of the new low-GWP refrigerants R1234ze(Z) and R1233zd(E) inside a small commercial brazed plate heat exchanger”, Int. J. Refrigeration, Vo. 104, 2019, 376-385.